

Quantification of Aortic Motion in Wild-Type and Apolipoprotein E-Deficient Mice Using Time Resolved MR Angiography: Possible Correlation between Direction of Vessel Motion and Abdominal Aortic Aneurysm Bulging

C. J. Goergen¹, M. Hedeus², C. A. Taylor¹, P. S. Tsao³, and J. M. Greve²

¹Bioengineering, Stanford University, Stanford, CA, United States, ²Biomedical Imaging, Genentech Inc., South San Francisco, CA, United States, ³Cardiovascular Medicine, Stanford University, Stanford, CA, United States

Introduction

Arterial wall biomechanics are thought to be important in localization, initiation, and progression of cardiovascular disease. Abdominal aortic aneurysm (AAA), defined as at least a 1.5-fold increase in vessel diameter, leads to approximately 15,000 deaths per year in the United States and has well-known clinical morbidities. However, a detailed understanding of the underlying mechanisms that lead to initiation of the disease and progressive expansion of the vessel remain elusive. As a way to better understand the human condition, murine AAA models have been developed. Aneurysm research in mice to date has been limited to using invasive or 2D ultrasound methods to assess vessel growth and have not considered wall dynamics. While using MRI to observe disease progression in the angiotensin II (angII)/apolipoprotein E-deficient (apoE^{-/-}) model,¹ we noticed repeatable and significant directionality in the shape of these AAAs (i.e. leftward expansion directly above the right renal artery, Figure 1).² Previous research has shown that the stress within the wall of an AAA, and possibly the potential for rupture, are as dependent on aneurysm shape as they are on maximum diameter.³ As clinical and animal studies have shown that the aorta undergoes non-uniform circumferential deformation throughout the cardiac cycle,^{4,6} we hypothesized that the direction of aortic motion may influence AAA shape. The purpose of this study was to develop high spatial and temporal resolution MR imaging methods to characterize wall motion and aortic displacement of mouse aortas, with the future goal of comparing the motion of healthy vasculature to the direction of AAA bulging.

Materials and Methods

All experiments were conducted with local Institutional Animal Care and Use Committee approval. Male 24-41 week old C57/Bl6 (wild-type or WT) and apoE^{-/-} (C57/Bl6 background) mice were used. MRI was performed at 4.7T using a Direct Drive console (Varian, Inc., Palo Alto, CA). A 2D time-of-flight sequence was used to quantify lumen expansion throughout the cardiac cycle (TR/TE 106-126/4ms depending upon heart rate, FOV (2cm)², alpha=20°, matrix 128² zero-filled to 256², slice thickness 2mm, NEX 8, 11 cine frames, 4cm transmit-receive volume coil, apoE^{-/-} n=9, WT n=9). Maximum intensity projections from a 3D time-of-flight sequence were used to plan 2D slices at the supraceliac (SC) level, at the suprarenal (SR) level, at the infrarenal (IR) level, and above the iliac and tail trifurcation (supratrifurcation-Stri). A 20mm saturation band was placed 2mm below the slice of interest to remove signal from venous flow (alpha=90°). Two subcutaneous ECG leads and a respiratory monitor (SA Instruments, Inc., NY) were utilized for prospective triggering off of the R-wave only during exhalation. Mice were anesthetized using isoflurane, and body temperature was maintained from 36-37°C. The boundary of the aorta in each frame was defined using thresholding or manual segmentation with SimVascular.⁷ Ultrasound (US) was used to verify *in vivo* wall motion measurements at the supraceliac level with an axial projection (transducer 707B, Vovo 770, VisualSonics, Toronto, Canada). An ANOVA with a Scheffe post-hoc test was used for significance ($p<0.05$ for significance; Matlab, MathWorks Inc., Natick, MA).

Results

Circumferential cyclic Green-Lagrange strain was calculated as $\varepsilon_{\text{cp}}=1/2[(P/P_{\text{min}})^2-1]$, where P is the perimeter of the aorta at the time of interest, and P_{min} is the minimum perimeter throughout the cardiac cycle. Strain curves at all four locations for both apoE^{-/-} and WT mice can be seen in Figure 2. Similar results are seen between MR and US measurements in the SC location, and between apoE^{-/-} and WT mice at all four locations. The coordinates of the centroid from each segmentation were also calculated, with the magnitude and direction of motion shown in Table 1. The centroid of the vessel at the SC and SR locations moved a significantly greater distance than the IR and Stri locations ($p<0.05$). The direction of this motion was also significantly different above and below the renal arteries; SC and SR segments moved from right to left, while IR and Stri segments moved posterior to anterior ($p<0.001$).

Discussion

The data presented in this study suggest that aortic dynamics differ greatly above and below the renal arteries in mice. Similar cyclic strain waveforms from WT and apoE^{-/-} mice at all four locations are not unexpected as the transgenic mice were bred on a C57/Bl6 background. Comparison of our MR data to US measurements at the SC level (waveforms in Figure 2a) and from the literature give us confidence that our technique accurately measures luminal expansion.⁶ The highly different directions of motion are likely due to anatomical differences between the infrarenal and suprarenal aorta. The spine, muscle, stomach, and branching vessels could all influence the direction of motion of the aorta. Of note is the strong leftward directionality of the SR region, precisely where we observed leftward expansion in the angII/apoE^{-/-} mouse AAA model. The results of this study suggest a relationship between the direction of aortic motion and the shape of these AAAs.

Acknowledgements: The authors would like to thank Jed Ross, Nathan Wilson, and Prahallad Iyengar for their technical assistance. Funding for CJG was provided by an American Heart Association Predoctoral Fellowship (0815293F).

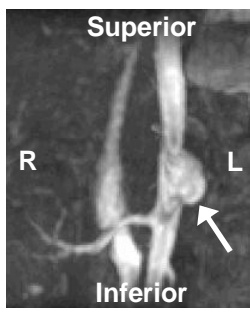
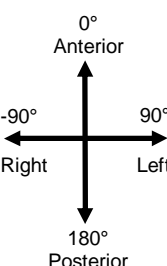


Figure 1 – Murine suprarenal AAA (arrow).

Table 1 – Magnitude and direction of centroid motion throughout the cardiac cycle. Anterior motion was defined as 0°, with positive angles to the anatomical left. Data shown as mean±SD.

Centroid Motion		Mag. (μm)	Angle (deg)
SC	ApoE ^{-/-}	89.9 ± 38.9	89.1 ± 11.6
	WT	110.4 ± 23.8	89.4 ± 10.7
SR	ApoE ^{-/-}	145.2 ± 27.1	85.7 ± 10.5
	WT	101.0 ± 20.3	83.9 ± 13.9
IR	ApoE ^{-/-}	37.4 ± 17.5	-20.9 ± 25.8
	WT	47.1 ± 12.3	-17.6 ± 24.5
Stri	ApoE ^{-/-}	33.5 ± 11.9	-18.1 ± 40.1
	WT	29.2 ± 14.8	-3.3 ± 40.7



References

- Daugherty A et al., *J Clin Invest* 105, 1605 (Jun, 2000).
- Goergen CJ et al., presented at the ASME 2008 SBC, Marco Island, FL (Jun 25-29, 2008).
- Vorp D, et al., *J Vasc Surg* 27, 632 (Apr, 1998).
- Draney MT et al., *Magn Reson Med* 52, 286 (Aug, 2004).
- Draney MT et al., *Ann Biomed Eng* 30, 1033 (Sep, 2002).
- Goergen CJ et al., *J Endovasc Ther* 14, 574 (Aug, 2007).
- <https://simtk.org/home/simvascular>

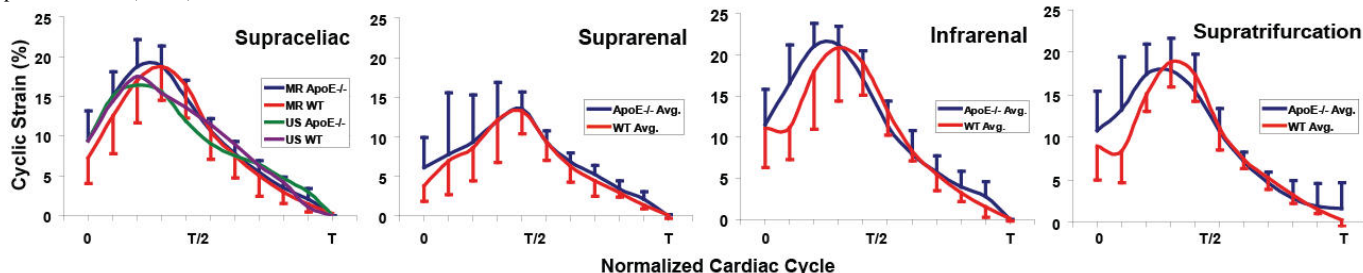


Figure 2 – Circumferential cyclic strain over a normalized cardiac cycle for apoE^{-/-} and WT mice (US data also shown at SC location). Curves represent mean±SD.